Formation of ultra-compact dwarf galaxies: tests of the galaxy threshing scenario in Fornax

P. A. Thomas,[1]⋆ M. J. Drinkwater[2] and E. Evstigneeva[2]

[1]*Astronomy Centre, University of Sussex, Falmer, Brighton BN1 9QH*
[2]*Department of Physics, University of Queensland, QLD 4072, Australia*

ABSTRACT

This paper investigates the possibility that ultra-compact dwarf (UCD) galaxies in the Fornax cluster are formed by the threshing of nucleated, early-type dwarf galaxies (hereafter dwarf galaxies).

Similar to the results of Côté et al. for the Virgo cluster, we show that the Fornax cluster observations are consistent with a single population in which all dwarfs are nucleated, with a ratio of nuclear to total magnitude that varies slowly with magnitude. Importantly, the magnitude distribution of the UCD population is similar to that of the dwarf nuclei in the Fornax cluster.

The joint population of UCDs and the dwarfs from which they may originate is modelled and shown to be consistent with a Navarro, Frenk & White (NFW) profile with a characteristic radius of 5 kpc. Furthermore, a steady-state dynamical model reproduces the known mass profile of Fornax. However, there are a number of peculiarities in the velocity dispersion data that remain unexplained.

The simplest possible threshing model is tested, in which dwarf galaxies move on orbits in a static cluster potential and are threshed if they pass within a radius at which the tidal force from the cluster exceeds the internal gravity at the core of their dark matter halo. This fails to reproduce the observed fraction of UCDs at radii greater than 30 kpc from the core of Fornax.

Key words: methods: analytical – galaxies: dwarf – galaxies: formation.

1 INTRODUCTION

In recent years, considerable evidence has been accumulated regarding the fact that disruptive processes play an important role in galaxy evolution as well as the more dominant hierarchical merging. Observational evidence for these disruptive processes is particularly evident in the dense environment of galaxy clusters. The evidence includes populations of individual intra-cluster objects such as planetary nebulae (Arnaboldi et al. 2004; Feldmeier et al. 2004a) and red giant stars (Durrell et al. 2002), as well as the general diffuse light now thought to make up a significant fraction of the total stellar mass in clusters (Feldmeier et al. 2004a,b; Gonzalez, Zabludoff & Zaritsky 2005; Zibetti et al. 2005).

In this paper, we focus on a relatively new component of intra-cluster space, ultra-compact dwarf (UCD) galaxies. These are compact systems of old stars akin to globular clusters but they are 10–100 times more luminous than Galactic globular clusters and they are located in intra-cluster space between galaxies. The first

UCDs were discovered in the Fornax cluster independently in studies of globular clusters (Minniti et al. 1998; Hilker, Infante & Vieira 1999) and in studies of compact dwarf galaxies (Drinkwater et al. 2000b; Phillipps et al. 2001). The UCDs are unlike any known galaxies in terms of luminosity, morphology and size (Drinkwater et al. 2003). Several hypotheses have been suggested to explain the origin of UCDs ranging from them being the high-luminosity end of a putative intra-cluster globular cluster distribution to being the evolved super-star clusters formed in galaxy merger events. In this paper, we focus on the model that UCDs are formed by the global tidal field of a cluster which can strip, or 'thresh', the outer stellar envelopes of nucleated dwarf galaxies (dE, Ns and dS0, Ns) as they pass repeatedly through the inner regions of a cluster leaving just the bare nucleus to survive as a UCD (Bekki, Couch & Drinkwater 2001; Bekki et al. 2003; Goerdt et al. 2008).

The motivation for the current work is the subsequent discovery of a larger population of fainter UCDs in the central region of the Fornax cluster (Drinkwater et al. 2004; Gregg et al. 2008). This sample of 60 UCDs is large enough to permit us to test several aspects of the threshing hypothesis using a statistically significant sample. Our focus will be to test simple aspects of the distributions of the

⋆E-mail: p.a.thomas@sussex.ac.uk

UCD and galaxy populations. An alternative approach based on the internal properties of the UCDs is also in progress (e.g. Evstigneeva et al. 2007).

Our basic premise for this paper is that if UCDs are descendants of disrupted galaxies, then the UCD parent population can be modelled by the combined *current* population of Fornax cluster UCDs and dwarf galaxies. We test whether the observed spatial and velocity distributions of the two populations are consistent with this hypothesis and conclude that they are. We then model the orbits of UCDs/galaxies drawn from this joint population to determine what fraction of them passes close enough to the cluster centre to lead to threshing. The relative fraction UCDs to dwarfs seen at large radii in Fornax is inconsistent with this static threshing model.

In Section 2, we define the UCD and galaxy samples for our analysis. In Section 3, we test if the luminosity function of the UCDs is consistent with them having been drawn as random sample from the nuclei of dwarf galaxies in the cluster. Section 4 develops a dynamical model for the joint population, and Section 5 calculates the fraction of threshed orbits at each radius. Finally, in Section 6, we summarize our results and draw conclusions about the plausibility of the threshing hypothesis.

We adopt a distance of 20 Mpc to the Fornax cluster (Drinkwater, Gregg & Colless 2001a) corresponding to a distance modulus of 31.51 mag. In this paper, we are not concerned with late-type galaxies. To avoid endless repetition, we use the terms galaxy and dwarf to refer to early-type objects only, as defined in Section 2.1.

2 DATA SAMPLES FROM THE FORNAX CLUSTER

2.1 Early-type galaxy sample

The hypothesis that we test in this paper is that UCDs form from the disruption of nucleated dwarf galaxies. Our authority for the morphological classification of Fornax cluster galaxies is the *Fornax Cluster Catalogue* (FCC; Ferguson 1989) which was based on photographic data. The FCC lists some 291 galaxies as early types (i.e. not Sa-d, Sm or Im; we include spheroidal galaxies in our sample). Of these, 103 are classified as nucleated. Recent *Hubble Space Telescope* (*HST*) imaging results from the ACS Virgo Cluster Survey (Côté et al. 2006, hereafter CPF06) suggest that the frequency of nucleation in early-type galaxies is actually much higher than suggested from the photographic ground-based surveys. Faint nuclei are difficult to detect because they are washed out by atmospheric seeing, and the central regions of the brightest galaxies are saturated. Notably, CPF06 suggest that potentially *all* dwarf galaxies may contain nuclei. We apply the CPF6 model to our Fornax data in Section 3.1 and show that the observed fraction of nucleated dwarfs as a function of magnitude is consistent with this assumption. Also, the spatial distributions of nucleated and non-nucleated dwarfs, shown in Fig. 4, are indistinguishable.

For the purposes of this current work, therefore, we define the parent galaxy sample to be all early-type dwarf galaxies listed as definite or probable members in the FCC. Where radial velocities are known, we use these to define membership, otherwise we use the FCC membership classifications. New radial velocities result in the removal of some FCC-classified members and the inclusion of some FCC-classified background galaxies, now known to be members (e.g. see Drinkwater et al. 2001b). More recent radial velocity measurements are taken from Karick, Drinkwater & Gregg (2003). Where the classification is uncertain, we have taken all galaxies fainter than $M_B = -14$ as dwarf; the maximum magnitude for a

Table 1. Spectroscopic completeness of the UCD sample. Completeness, C, is defined as the fraction of UCD targets for which redshifts were measured. N_{UCD}, in two bins of projected radius r, is the number of UCDs found in each magnitude range. The actual number of UCDs can therefore by estimated as N_{UCD}/C.

b_J range	M_B range	C	N_{UCD}	
			$r < 17.5$ kpc	$r > 17.5$ kpc
16.0–20.5	−15.3 to −10.8	0.94	0	21
20.5–21.0	−10.8 to −10.3	0.81	6	14
21.0–21.5	−10.3 to −9.8	0.35	5	14

normal galaxy is then $M_B = -16.3$ and the minimum magnitude for a dwarf galaxy is $M_B = -17.8$. A complete list of the galaxies is given in Table A1.

The galaxies in our sample have morphological classifications from the FCC which can include a flag to show that they are nucleated. We use these flags in our discussion below, but we emphasize that there is no *HST* imaging for most of these galaxies, so we cannot tell with certainty if a given galaxy is really nucleated. We instead adopt the general result of CPF06 that all dwarf galaxies have nuclei, with a magnitude that is related to that of the host galaxy (see Section 3.1).

The dwarf galaxy sample that we use is effectively complete to a limit of around $M_B = -13.5$ (see FCC). The velocity data used to confirm cluster membership are complete for galaxies brighter than $M_B = -16$ and become 50 per cent complete at $M_B = -14.5$.

2.2 UCD sample

The UCDs were originally discovered as part of the all-object Fornax Cluster Spectroscopic Survey (Drinkwater et al. 2000a). Although the original survey measured all objects (to $b_J < 19.8$), this was subsequently extended in a selective search at fainter limits specifically designed to find UCDs. The selected search used a slightly smaller field: a radius limit of 0°.9 (314 kpc) around the central cluster galaxy NGC 1399. The selected search also used a restricted colour range of $b_J - r_F < 1.7$ for objects with both b_J and r_F values measured; for fainter objects with no r_F values, no colour criterion was applied. This colour selection served to remove Galactic M-dwarf stars from the sample: no UCDs have colours in this range. The completeness of the spectroscopic observations is given as a function of magnitude in Table 1.

The b_J photographic APM magnitudes were converted to m_B magnitudes by the approximate relation $m_B = b_J + 0.20$ [based on the Blair & Gilmore (1982) relation of $b_J = B - 0.28(B - V)$ for an average dwarf galaxy colour of $B - V = 0.7$] so that $M_B = b_J + 0.20 - 31.51 = b_J - 31.31$.

The spatial locations of the UCDs are far from circularly symmetric about the centre of Fornax but tend to lie in a band running from northeast to southwest (see fig. 2 in Gregg et al. 2008). This presumably reflects the infall pattern on to the cluster. Provided that the distribution is relaxed, this will not affect the dynamical modelling; however it may confuse the relation between the true three-dimensional positions and velocities and the observed ones. For the purposes of modelling in this paper, we assume a spherically symmetric distribution.

2.3 Joint sample selection

According to our central hypothesis, there was an original parent population of dwarf galaxies, some of which were subsequently
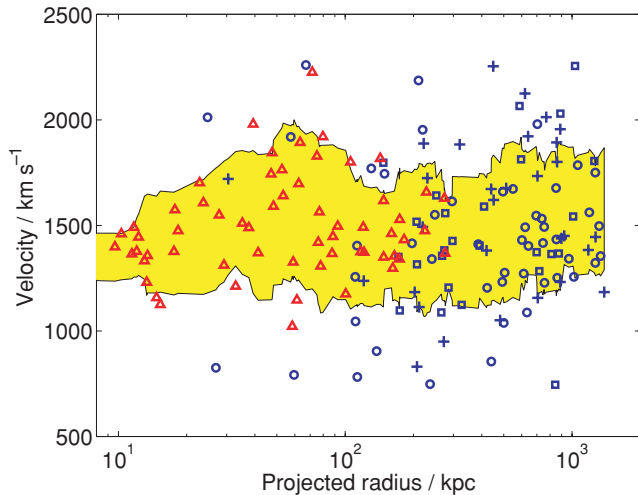
Figure 1. A comparison of the UCD and galaxy populations. The radial velocities are plotted as a function of projected radius. UCDs are shown as red triangles, normal galaxies as blue squares, and dwarfs brighter and fainter than $M_B = -15.0$ as blue circles and crosses, respectively. The yellow shaded area shows a running mean of the 1σ velocity dispersion.

Table 2. Number of Fornax galaxies of different types in different annular bins centred on NGC 1399. The division between bright and faint dwarfs is taken as $M_B = -15.0$.

Sample	Radial range in kpc		
	17.5–314	314–1 050	1 050–1 500
UCDs	49	0	0
Normal galaxies	13	13	4
Bright dwarfs	11	22	5
Faint dwarfs	65	129	28

3 COMPARISON OF LUMINOSITY DISTRIBUTIONS

In this section, we develop a unified model for nucleated and non-nucleated dwarf galaxies whereby all galaxies have nuclei but only a fraction of these are bright enough to be detected and classified as such in the FCC. We then go on to compare the predicted luminosity function of nuclei with that of UCDs. As we are interested only in the shape of the magnitude distributions, we use the full samples of dwarfs and UCDs even though two extend over different spatial regions.

3.1 Early-type nuclei

An important property of the parent galaxies is the luminosity distribution of the galaxy nuclei as these will be compared to the UCD luminosities. We cannot directly measure the luminosities of galaxy nuclei in the Fornax cluster because most do not have high-resolution *HST* imaging. Instead, we take a statistical approach: we assume that *all* dwarf galaxies host nuclei and infer the nuclear luminosities from the total galaxy luminosities.

CPF06 measured nuclear luminosities for 51 dwarf galaxies in the Virgo cluster. They confirmed previous suggestions that the nuclear luminosities increase with the galaxy luminosity. They modelled this relation as both a fixed offset between the nuclear and total magnitudes, $g'_{\rm nuc} = g'_{\rm gal} + (6.25 \pm 0.21)$, and an offset slowly varying with magnitude, $g'_{\rm nuc} = (0.90 \pm 0.18)\, g'_{\rm gal} + (7.59 \pm 2.50)$. We note that our galaxy sample extends to much fainter magnitudes than did the Virgo sample studied by CPF06, and so we will have to extrapolate their relation. We therefore allow the slope of the relation to vary, but require that it go through the mid-point of the CPF06 data ($g'_{\rm gal}, g'_{\rm nuc} = 13.40, 19.65$) defined by the crossing point of their two relations.

We model the scatter in the relationship by adding a random normal variable with a mean of zero and a standard deviation of 1.5 to the derived nuclear magnitude. The standard deviation was inferred from the scatter about the fixed-slope fit of CPF06 (their equation 15).

To convert the ACS g' photometry to absolute magnitudes, we first use the mean value of $B_T - g = 0.30$ for the ACS dwarf galaxies to convert g magnitudes to B_T. We then apply the distance modulus of 31.09 mag quoted by CPF06, obtaining $M_B = g' - 30.79$.

To constrain the slope of the $g'_{\rm nuc}$–$g'_{\rm gal}$ relation, we require that it predicts the correct distribution of galaxies that we would expect to have been classified as nucleated in the photographic FCC survey. For each galaxy, we predict its nuclear luminosity as above, then we classify it as nucleated if the nucleus is brighter than the point-source detection limit on the photographic plate (approximately $B_T = 22.6$ or $M_B = -8.9$ for the FCC; H. Ferguson, private communication).

The results, shown in Fig. 2, show that this model can nicely predict the luminosity distribution of the early-type galaxies that
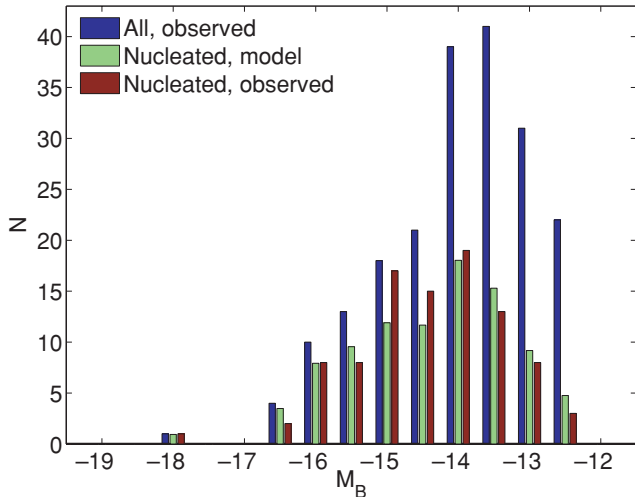
disrupted to form UCDs. Unfortunately, the selection effects are different for the two sub-populations and so we need to use different samples for different parts of our analysis. This will be described at the beginning of each relevant section. Here, we make a few general comments on the relative spatial extent of the dwarf and UCD samples.

The FCC is a wide-field survey. It covers a rectangular region with a largest inscribed circle that extends to a radius of $3°$ (1.05 Mpc) from the cluster centre. Our main UCD sample is limited to a smaller region defined by a maximum radius of $0°.9$ (314 kpc) from the cluster centre. We have modelled the density distribution and estimate that there may be up to six missing UCDs at larger radii (although, for the brighter UCDs, two additional regions extending to a radius of $3°$ have been surveyed and no UCDs were found). Adding six extra UCDs with the appropriate density distribution makes very little difference to the modelling of the spatial distribution of the joint UCD plus dwarf population in Section 4.1.

For the UCDs, there is also a need to exclude those at very small radii from the central cluster galaxy, NGC 1399. The distribution of UCD radial velocities shown in Fig. 1 shows a trend to smaller velocities (and velocity dispersion) at low radius. The inner UCDs are clearly moving in the galactic and not the cluster potential and could be considered as bright globular clusters attached to NGC 1399. The choice of where to draw the dividing line between galactic and intracluster UCDs is somewhat arbitrary. We cut at 3 arcmin (17.5 kpc) which excludes 11 UCDs from our sample (see Table 1), including the two relatively low velocity UCDs seen in the figure at a radius and velocity of approximately 15 kpc and 1140 km s^{-1}, respectively. (Including these two in our analysis makes little difference to the results and would leave the velocity dispersion of the excluded clusters as formally zero once the velocity errors have been accounted for.)

For reasons that we will describe in Section 3.2, we divide the dwarf population into two. 'Bright dwarfs' with $M_B < -15.0$ are those that correspond to the progenitors of UCDs in our model, whereas 'faint dwarfs' would give UCDs that fall below our magnitude limit. Table 2 gives the number of galaxies of each type in different radial bins.

Figure 2. The distribution of dwarf galaxies classified as 'nucleated'. The leftmost, blue bars show the observed magnitudes of all Fornax dwarfs. The middle, green bars show only those whose predicted nuclear magnitudes would be greater than -8.9 according to the model developed in the text. Finally, the rightmost, brown bars show the actual magnitude distribution of nucleated dwarfs in Fornax.

Figure 3. The leftmost, blue bars show the predicted distribution of nuclear magnitudes for Fornax dwarfs, averaged over 100 realizations: the middle, green bars multiply this by the completeness factor for UCD observations. If the threshing hypothesis is correct, then this should be proportional to the rightmost, brown bars that show the observed distribution of UCD magnitudes.

are classified as nucleated in the photographic FCC survey. To produce the figure, we used a slope of 0.7, smaller than the best fit of CPF06.[1] The nuclear-to-total magnitude relation becomes

$$M_{B\,\mathrm{nuc}} + 11.14 = 0.7(M_{B\,\mathrm{gal}} + 17.39). \tag{1}$$

The leftmost, blue bars in the figure show the magnitude distribution of all dwarfs. We averaged over 100 realizations of the scatter in the relation to obtain the prediction for observable, nucleated dwarfs shown in the green, middle bars of the figure. These are statistically indistinguishable from the actual number of dwarfs classified as nucleated, shown in the rightmost, brown bars.

We show in Section 4.1 that the spatial distributions of the nucleated and non-nucleated dwarfs are identical, thus lending further support to the hypothesis that the presence of a detectable nucleus is the only difference between them.

3.2 UCDs

From the observed dwarf population, we can now predict the distribution of nuclear magnitudes. If we assume that the threshing process is independent of galactic (and nuclear) luminosity, then these should have the same *shape* of distribution as the UCDs. Furthermore, the relative normalization should tell us what fraction of the dwarfs has been threshed. The predicted and actual UCD distributions are given in Fig 3. Note that the predicted numbers from our model have been scaled down by the completeness values in Table 1 to allow for the fraction of unmeasured objects.

---

[1] It is not clear as to whether the CPF06 data will accept a slope of 0.7: we can also get an acceptable fit if we use a slope of 0.9 for the relation, provided that the magnitude limit for point-source detection is raised to -8.5.

If we extend our analysis to include normal galaxies, then we predict far more nucleated galaxies than are observed. This seems to be in disagreement with the results from Virgo; however, it is possible that bright nuclei would be saturated on the photographic plate and so are hard to detect: we note that CPF06 find many more nuclei in bright galaxies with $M_B \le -17.4$, than did photographic surveys.
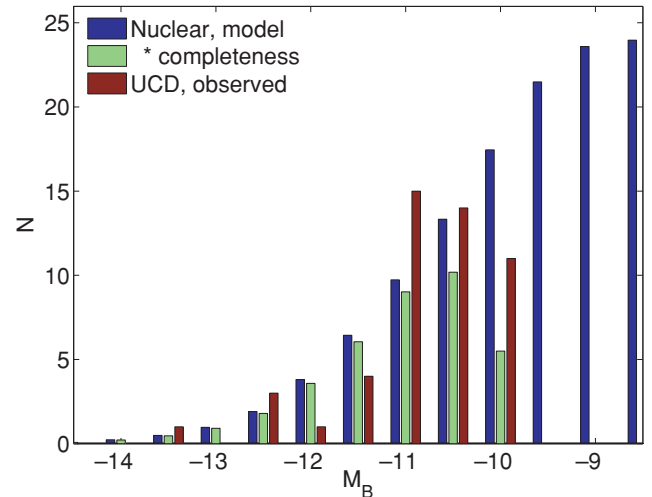
The figure shows that the predicted luminosity distribution of UCDs is not perfect. The model seems to give an excess of UCDs brighter than $M_B = -11.25$ as compared to fainter ones. It is hard to assess the significance of this: given the relatively small number of objects and the uncertainties in the relationship between galactic and nuclear magnitudes, it is probably acceptable.

The model predicts that 38 dwarfs should have nuclei that correspond to observable UCDs. This motivates our selection of $M_B = -15.0$ as the dividing line between bright and faint dwarfs, as this gives 38 bright dwarfs. Without scatter, equation (1) would have predicted a brighter limit, $M_B \approx -15.8$, but the greater number of faint galaxies biases things towards fainter magnitudes. Of these 38 dwarfs, only 11 lie within 314 kpc. Thus, the model predicts that the vast majority of dwarfs within this region are likely to be threshed. Even when averaged over the whole sample, more than half the dwarf population should be threshed.

4 A DYNAMICAL MODEL FOR THE JOINT DWARF/UCD POPULATION

This section constructs a model of the three-dimensional density distribution of the joint dwarf/UCD population in the cluster. There will turn out to be some degeneracy in the models which we will attempt to constrain by matching them to observed mass models for Fornax.

When comparing dwarfs and UCDs, we restrict our attention to the bright dwarfs, $M_B < -15.0$, as described in the previous section. We will show that the joint UCD + bright dwarf population is well fitted by an Navarro, Frenk & White (NFW) model (Navarro et al. 1997) in dynamical equilibrium in the cluster potential.

4.1 Spatial distributions

We first compare the spatial distribution of nucleated and non-nucleated dwarfs. If we plot all the dwarf galaxies together, as in Fig. 4, the nucleated dwarfs are shown to be very slightly more centrally concentrated. This is in the same sense as was originally
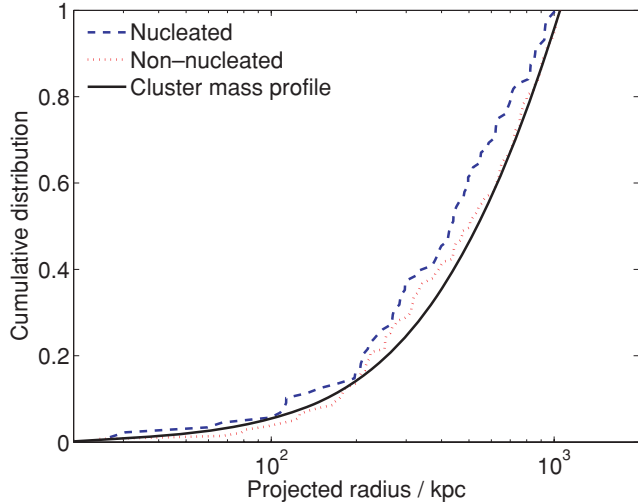
Figure 4. The cumulative numbers of nucleated (dashed, blue) and non-nucleated (dotted, red) dwarf galaxies in Fornax as a function of projected radius between 17.5 and 1050 kpc. Shown also as a solid, black line is the cluster mass profile described in Section 4.3.

Figure 5. The cumulative numbers of normal galaxies (dash–dotted, blue), bright dwarfs (dotted, red), faint dwarfs (dashed, green) and UCDs (solid, black) in Fornax as a function of projected radius between 17.5 and 1050 kpc. We have adjusted the normalization of the UCD curve to match that of the dwarfs at 314 kpc.

reported for the dwarf galaxies of the Virgo (Binggeli, Tammann & Sandage 1987) and Fornax (Ferguson & Sandage 1989) clusters, but for our present sample the difference is not significant (the Kolmogorov–Smirnov test returns a probability that the two are drawn from the same distribution of 0.2.). As expected from our above discussion, the nucleated dwarfs are significantly more luminous on average than the non-nucleated dwarfs: the difference in radial distributions is actually a luminosity bias. If, instead, we compare the distributions of dwarfs of the same luminosity ($M_B > -15$), then the difference is removed entirely. This observation strengthens the hypothesis of the previous section that dwarfs classified as nucleated or non-nucleated may differ only in the detectability of their central nucleus.

Also shown in the figure is the observed mass profile of the Fornax cluster, as described in Section 4.3. The cumulative number density profile of the dwarfs matches that of the cluster mass profile very well and shows no evidence of dwarf galaxy disruption near the cluster core.

Next, in Fig. 5 we compare the radial distributions of normal galaxies, bright and faint dwarfs and UCDs. Because the UCD survey extends only out to 314 kpc, we have adjusted the normalization of the cumulative distribution to match that of the dwarfs at this radius.

It is immediately obvious that the different populations show different degrees of central concentration. Notably, within 314 kpc, the radial distribution of the faint dwarfs is significantly more extended than that of both the bright dwarfs and the UCDs. At first glance, this appears to be at odds with the threshing model developed below (Section 5.1). The model suggests that faint dwarfs are more compact and therefore less likely to be threshed than bright ones, but we have not looked for UCDs at magnitudes corresponding to the faint dwarfs so we cannot test the number that have been threshed. Conversely, we do not see a significant difference between the distributions of UCDs and bright dwarfs, although we would expect the UCDs to be more centrally concentrated than the (surviving) dwarf galaxies according to our model. In this case, the relatively small number of objects involved may explain why the difference is not significant.
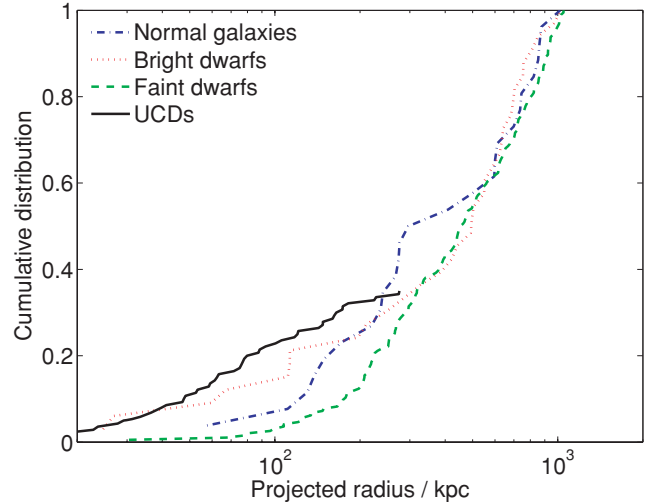
Outside 314 kpc, the distributions of bright and faint dwarfs are indistinguishable. There are hints that the UCD distribution is flattening between 200 and 314 kpc and no UCDs have been detected in (incomplete) observations in a few fields beyond this radius. For the purposes of the modelling that follows, we therefore assume that there are no UCDs with cluster-centric radii exceeding 314 kpc. If there are any, the number density of dwarfs rises so rapidly in this region that the latter would dominate anyway.

We plot the radial distribution of normal galaxies just for interest. The numbers are so few that it is formally indistinguishable from either the bright or faint dwarf population. We note, however, that it is significantly less centrally concentrated within 314 kpc than the UCD population.

Assuming a spherically symmetric distribution dependent only on radius, r, we model the density, $\rho(r)$, with profiles of the form

$$\rho = \frac{\rho_0}{x \, (1+x)^{s-1}}, \tag{2}$$

where $x = r/a$, and a and s are fitting parameters. (We fit only for the shape of the distribution: the normalization ρ_0 can be chosen so as to match the correct number of objects.) We project each distribution on to the sky and then compare the predicted cumulative mass profile as a function of radius to the observed distribution, using the Kolmogorov–Smirnov test.

Fig. 6 shows the allowable range of parameters and Fig. 7 shows the best-fitting model, although there is a strong degeneracy between a and s such that a wide variety of fits are acceptable. We will show results for $s = 3.0$, $a = 5$ kpc and for $s = 4.0$, $a = 90$ kpc; both lead to very similar conclusions.

4.2 Velocities

The velocity dispersions for different sub-samples of Fornax UCDs and galaxies are shown in Table 3. To determine the population velocity dispersions, σ, we used the following formula:

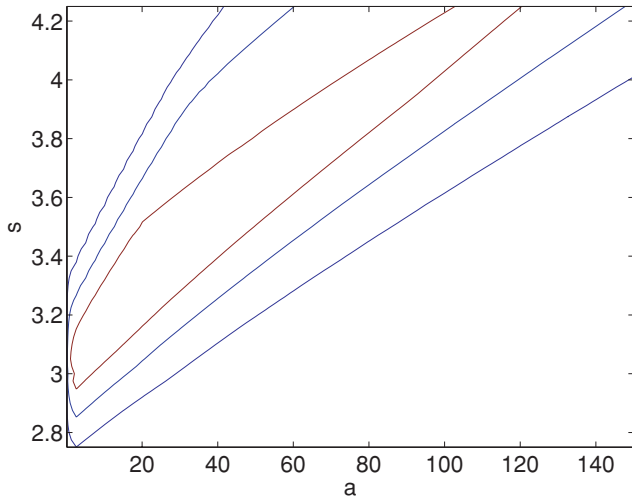$$\sigma^2 \sum_i w_i = \sum_i w_i \left[(v_i - \bar{v})^2 - \sigma_{e,i}^2 \right], \tag{3}$$

Figure 6. The 1σ, 2σ and 3σ range of allowable parameters in the fit to the joint UCD plus bright dwarf population.
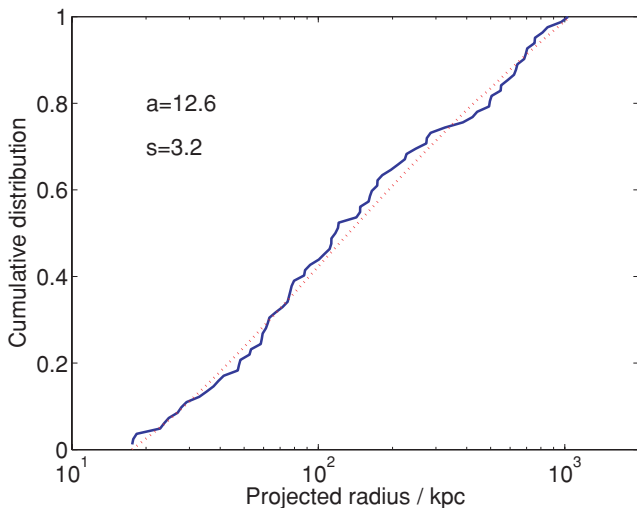

Figure 7. The best-fitting cumulative profile of the total number of UCD+bright dwarf galaxies as a function of projected radius: (solid, blue) data, (dotted, red) model.

where v_i and $\sigma_{e,i}$ are the observed velocities and their rms measurement errors, respectively, $\bar{v}$ is the mean velocity for the full sample of all galaxies plus UCDs outside 17.5 kpc,

$$\bar{v} \sum_i w_i = \sum_i w_i v_i, \qquad (4)$$

and

$$w_i = \frac{1}{\sigma^2 + \sigma_{e,i}^2} \qquad (5)$$

are weights chosen so as to maximize the information in the data.[2]

The low-velocity dispersion of UCDs as compared to other galaxies is expected in the threshing model, because the UCDs are more

---

[2] We do not have any formal proof of this but note that the weights are equal when $\sigma_{e,i} \ll \sigma$ and tend to the known optimal weighting $w_i \propto 1/\sigma_{e,i}^2$ when $\sigma_{e,i} \gg \sigma$ (Irwin 1942). A similar, but not identical, expression is given by Pryor & Meylan (1993).

Table 3. Velocity dispersions for different subsamples of the UCD and galaxy populations in Fornax. The completeness of the velocity data can be found by comparing the numbers in this table with those in Table 2, but basically it is high except for the faint dwarfs. When calculating velocity dispersions for the different sub-samples, we have used the mean for the full sample of all galaxies (normal, dwarf and UCD) with radii greater than 17.5 kpc, $\bar{v} = 1491\,\text{km}\,\text{s}^{-1}$. The final column shows the rms error in the velocity dispersion measurements determined by bootstrap resampling 1000 times.

Sample	Number	$\sigma/\text{km}\,\text{s}^{-1}$		Error
		Raw	Corrected	
Full	154	321	316	19
UCDs + bright dwarfs	82	316	310	27
Normal	29	281	280	40
Bright dwarfs	33	401	399	42
Faint dwarfs	43	356	350	31
UCDs	49	235	224	29
UCDs, $17.5 < R/\text{kpc} < 76$	24	285	276	42
UCDs, $76 < R/\text{kpc} < 314$	25	174	159	28

centrally concentrated in the cluster potential (i.e. have a steeper density profile) – unfortunately, there are too few UCDs to quantify this. However, the table shows a number of other features that are hard to explain.

First, why is the velocity dispersion of normal galaxies so much smaller than that of dwarfs, and especially bright dwarfs, given that the two have similar radial distributions within the cluster? In Drinkwater et al. (2001a), this difference was interpreted as indicating that the dwarf galaxies were an unrelaxed, infalling, population. In this paper, we are assuming that all galaxies (including UCDs) are relaxed: an alternative explanation is that many of the dwarfs may be orbiting in bound subhaloes, with normal galaxies located at their centres.

Secondly, the line-of-sight velocity dispersion for UCDs is significantly higher at small radii than at large ones. Some difference of this kind would be expected if the UCDs are on preferentially radial orbits. Defining the velocity anisotropy parameter as $\beta = 1 - \sigma_t^2/\sigma_r^2$, where σ_r is the radial velocity dispersion with respect to the cluster centre and σ_t the tangential one, then this would correspond to $\beta > 0$. Unfortunately, the expected variation, calculated in Appendix B, is much too small to explain the observations. The observed decline in velocity dispersion between the inner and outer bin is 1:0.58. Even if we allow each measurement to move up to 1σ towards agreement (with probability less than 3 per cent), the ratio remains 1:0.80. This can only be explained with $\beta = 1$, corresponding to purely radial orbits. The explanation for this discrepancy may be related to the non-uniform distribution of UCDs within the Fornax cluster. If the outer UCDs have orbits that are preferentially moving perpendicular to the line-of-sight, then that would explain the effect.

Despite these uncertainties, we will model the joint UCD plus bright dwarf population as if it is relaxed. As we show in the next section, this provides a marginally acceptable fit to the known mass distribution in the Fornax cluster.

4.3 Cluster mass profile

The mass of Fornax has been investigated using a number of different techniques that probe different radial locations. Richtler et al. (2004) look at the dynamics of the globular cluster population
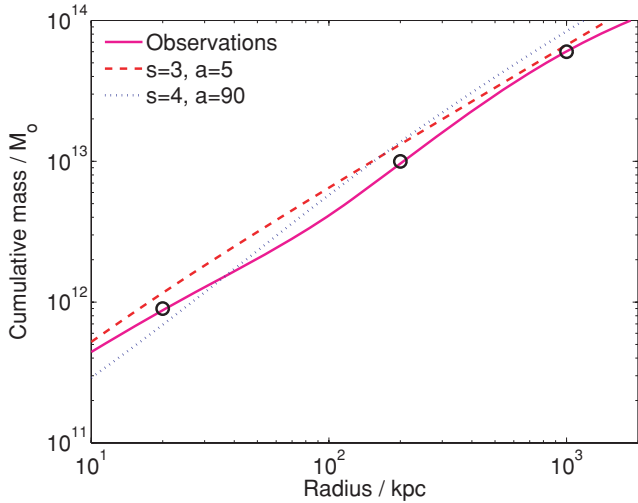
Figure 8. A comparison of the observed and modelled cluster mass profiles for the case of $\beta = 0$: observations (black circles and solid, magenta line), $s = 3, a = 5$ kpc (dashed, red line); $s = 4, a = 90$ kpc (dotted, blue line).

Figure 9. The predicted isotropic velocity dispersion profiles for the mass model given in equation (8) and for density profiles with parameters $s = 3$, $a = 5$ kpc (solid, red) and $s = 4, a = 90$ kpc (dotted, blue).

around NGC 1399. They find that

$$\frac{M}{M_\odot} \approx 4.5 \times 10^{10} \frac{r}{\text{kpc}} \tag{6}$$

for $r \lesssim 20$ kpc and increases in a similar vein to about twice this radius. This agrees with the *ASCA* observations of Ikebe et al. (1996) and the *ROSAT* observations of Jones et al. (1997). The two X-ray papers give different mass profiles at larger radii, but agree on a mass of 10^{13} $M_\odot$ within 200 kpc. Finally, Drinkwater et al. (2001a) have used the shape of the velocity cusp to determine a mass for the cluster as a whole of approximately 6×10^{13} $M_\odot$ within 1 Mpc.

We combine all these estimates into a density/mass model consisting of an inner truncated isothermal sphere centred on NGC 1399, plus a cluster NFW potential:

$$\rho = \frac{\rho_{BGC,0}}{x_{BCG}^2 \left(1 + x_{BCG}^2\right)} + \frac{\rho_{clus,0}}{x_{clus} \left(1 + x_{clus}\right)^2}; \tag{7}$$

$$M_r = M_{BCG} \frac{2}{\pi} \arctan x_{BCG}$$
$$+ M_{clus,0} \left[\ln(1 + x_{clus}) - \frac{x_{clus}}{1 + x_{clus}}\right], \tag{8}$$

where $M_{BCG} = 2\pi^2 a_{BCG}^3 \rho_{BCG,0} = 2.0 \times 10^{12}$ $M_\odot$; $a_{BCG} = 30$ kpc; $M_{clus,0} = 4\pi \rho_{clus,0} a_{clus}^3 = 1.1 \times 10^{14}$ $M_\odot$; $a_{clus} = 400$ kpc. Here, $\rho(r)$ is the density at clustocentric radius r, M_r is the mass contained within radius r, $x_{BCG} = r/a_{BCG}$ and $x_{clus} = r/a_{clus}$. Given the uncertainties in the observations, any other model that has $M \propto r$ in the centre, and that passes through the other mass points mentioned above, would be equally acceptable. The observational constraints are shown in Fig. 8 as black circles, and the model as a solid, magenta line.

If the joint UCD plus bright dwarf population is to be at rest in the cluster, then it must satisfy the Jeans equation:

$$\frac{1}{\rho} \frac{d\rho \sigma_r^2}{dr} + \frac{2\beta \sigma_r^2}{r} = -\frac{GM_r}{r^2}. \tag{9}$$

We can use this in two ways: to predict the mass distribution, given our dynamical model for the population, or to predict the velocity dispersion profile for the given observed mass profile.
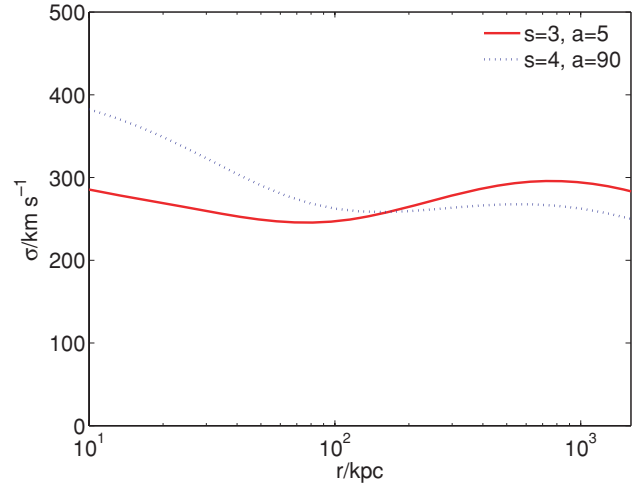
Fig. 8 shows a comparison between the observed mass profile and that predicted by two of the acceptable density models with constant velocity dispersion of 310 km s^{-1} and isotropic velocity dispersion tensors, $\beta = 0$. We have also tried models with $\beta > 0$. This makes very little difference to the $s = 3$ prediction but substantially worsens the $s = 4$ fit to the data at small radii.

Reversing this procedure, Fig. 9 gives the predicted velocity dispersion profile for a given density profile and observed cluster mass distribution. In making this prediction, we have taken the approximation that the logarithmic gradient in the velocity dispersion is small compared to that of the density. Once again, taking β to be greater than zero makes little difference to the $s = 3$ prediction, but worsens the $s = 4$ one, giving higher predicted velocity dispersion at small radii. In both these plots, the $s = 3$ curve provides the closer fit to the data. That it does not match every wiggle in the mass profile in Fig. 8 is not surprising given that the latter is somewhat arbitrary and that we have not allowed the velocity dispersion to vary with radius. The normalization is a little too high: lowering the velocity dispersion to 283 km s^{-1} would provide a very good fit to the mass profile. Given that this is only 1σ away from the measured value in Table 3, we regard this as marginally acceptable.

In Fig. 9, it may seem at first sight that the decline in velocity dispersion away from the core of the cluster mimics that seen in the UCD observations. However, a closer inspection reveals that the minimum in velocity dispersion seen in this plot lies at too small a radius and that by the edge of the UCD observations at around 300 kpc the velocity dispersion has risen to its central value.

5 A STATIC MODEL OF GALAXY THRESHING

In this section, we investigate the simplest threshing scenario in which dwarf galaxies orbit within the present-day Fornax cluster and are threshed if they pass close to the cluster core. We show that there are too many UCD galaxies at large radii for this model to be viable. We conclude that in any threshing model, disruption must occur near the cores of smaller subclumps, prior to cluster formation.

5.1 Threshing radii

To estimate the fraction of dwarf orbits at a given radius which lead to threshing, we calculate the probability for a galaxy with initial projected clustocentric radius and line-of-sight velocity to have $R_{min} < R_{th}$. Here, R_{min} is the minimum distance from the cluster centre during its orbit and R_{th} is the radius within which the stellar envelope of a nucleated dwarf can be removed by the tidal field of a cluster.

To determine R_{th} for a dwarf orbiting a cluster, we assume that R_{th} is the distance from the cluster centre at which the tidal force of the cluster equals the self-gravitational force of the dark-matter halo in the inner regions of the dwarf galaxy. This occurs at the clustocentric radius for which

$$\frac{GM_{dm}}{r_{dm}^2} = r_{dm} \left| \frac{d}{dr} \left(\frac{GM_{clus}}{r^2} \right) \right|, \tag{10}$$

where M_{dm} is the dwarf halo mass within radius r_{dm} and M_{clus} is the cluster mass profile from equation (8).

For the dark matter distribution in dwarf galaxies, we use a profile proposed by Burkert (1995):

$$\rho_{dm} = \frac{\rho_{dm,0}}{(1 + x_{dm})(1 + x_{dm}^2)}, \tag{11}$$

where $x_{dm} = r_{dm}/a_{dm}$, and $\rho_{dm,0}$ and a_{dm} are the central dark matter density and the core (scale) radius, respectively. This has an extended, constant-density central region within which

$$\frac{M_{dm}}{r_{dm}^3} \approx 4.19 \rho_{dm,0}, \tag{12}$$

so that M_{dm} and r_{dm} cancel in equation (10) leaving only a dependence upon $\rho_{dm,0}$. We note that the central mass profiles of dwarf galaxies are not very well known and could be more concentrated than assumed here. Were that to be the case, then the threshing radii would be reduced.

Burkert (1995) gives observed scaling relations between $\rho_{dm,0}, a_{dm}$ and the circular velocity, $v_{dm,0}$, at the core radius. At that radius, the velocity dispersion (assumed isotropic) is approximately $\sigma \approx v_{dm,0}/\sqrt{2}$ and we assume that this is close to the observed value for the dwarf as a whole. The relevant relation is then

$$\frac{\rho_{dm,0}}{M_\odot \, pc^{-3}} \approx 0.56 \left(\frac{\sigma}{km \, s^{-1}} \right)^{-1}. \tag{13}$$

For each UCD, we determine the most likely magnitude of its precursor dwarf using the relation of equation (1). We then use the observed relationship from Geha, Guhathakurta & van der Marel (2003) to relate the magnitude to velocity dispersion,

$$\log \left(\frac{\sigma}{km \, s^{-1}} \right) = 0.42 - 0.07 \, M_B. \tag{14}$$

This fixes the mean density within the core using equation (13), and we insert this in equation (10) to determine the threshing radius of any UCD as a function of its absolute magnitude. The results of these calculations are shown in Fig. 10.

Our approach in estimating the threshing radii is very similar to that used by Bekki et al. (2003) except for the following differences. First, we specifically use the local gradient of the cluster potential (rather than the point-mass assumption) and we add a core component to the cluster NFW potential. Secondly, we have used more recent scaling relations to derive the dwarf galaxy core masses as a function of their absolute magnitudes. Our estimates give very similar threshing radii: compare our Fig. 10 to their fig. 7.
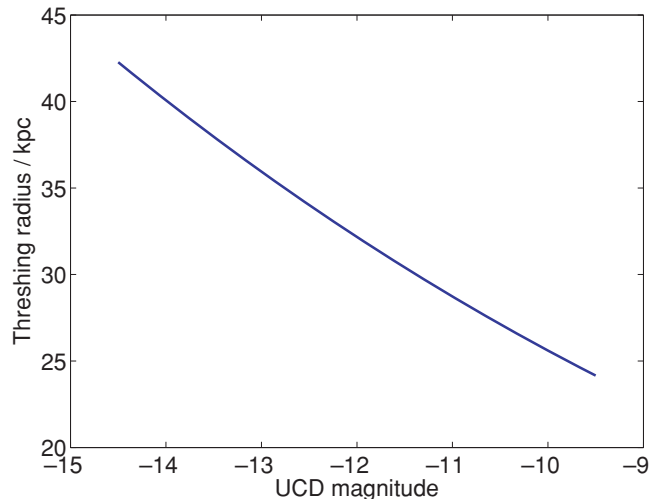

Figure 10. The predicted threshing radius as a function of UCD *B* magnitude.

Recently, Goerdt et al. (2008, hereafter GMK08) have conducted numerical simulations of threshing in a static potential similar to that of the Virgo cluster. They use two different models of a dwarf galaxy: one which consists solely of an extended dark matter halo with an NFW profile, and one in which this profile has been centrally concentrated by a dissipative baryonic disc. For the latter, the threshing radii they find are similar to ours. The dark-matter-only haloes can have much greater threshing radii, up to 200 kpc, but only for galaxies on quite circular orbits. As we discuss in Section 6, the two models bracket our predictions for UCD fractions as a function of radius, and both lead to the same qualitative results.

The detailed threshing simulations of individual dwarf galaxies by Bekki et al. (2003) showed that several pericentre passages within the threshing radius were necessary to completely strip the dwarf galaxy. In our model below, we do not count the number of orbits, but simply assume that any galaxy with an orbit that passes within its threshing radius will be stripped. This assumption is reasonable for galaxies within about 100 kpc of the cluster centre, but for those galaxies with radii of the order of 300 kpc, on the outskirts of the observed UCD distribution, there may have been only a single pericentric passage in the lifetime of the cluster. This could lead to an overestimate of the UCD fraction at large radii and would strengthen our results.

5.2 Galaxy orbits

The equation of motion for galaxy orbits in a spherically symmetric potential is

$$\ddot{r} - \frac{L^2}{r^3} = -\frac{GM_r}{r^2}, \tag{15}$$

where $L = rv_t = $ const is the specific angular momentum and v_t is the tangential component of the velocity.

Combining equations (9) and (15), multiplying by $\dot{r}$ and integrating lead to the following energy equation:

$$\frac{1}{2}\dot{r}^2 + \frac{1}{2}\frac{L^2}{r^2} - \sigma_r^2 \ln \left(\rho \sigma_r^2 \right) - 2\beta \sigma_r^2 \ln r = const, \tag{16}$$

where we have taken β to be constant and used the approximation that the gradient in σ_r^2 is much less than that in ρ and can be
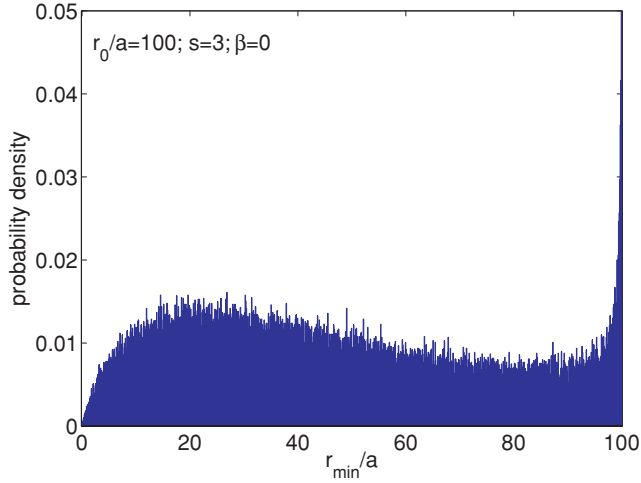
Figure 11. A histogram showing the probability density for the distribution of minimum orbital radii (pericentres) for a selection of galaxy orbits drawn from the appropriate Gaussian distribution of velocities. For this particular example, the one percentile of minimum radii is at $r_{\min} \approx 0.03 \, r_0$.

Figure 12. Comparison of observed and predicted fractions of UCDs. The circles show the observed UCD fraction (of the joint UCD plus bright dwarf sample) as a function of projected radius from the centre of the cluster. The lines show the predicted fraction of orbits that pass within the threshing radius of 30 kpc for $s = 3, a = 5$ kpc, $\beta = 0$ (solid, red), $s = 3$, $a = 5$ kpc, $\beta = 0.5$ (dashed, green) and $s = 4, a = 90$ kpc, $\beta = 0.$, (dotted, blue).

neglected. Putting in initial conditions (labelled with subscript 0) and setting $\dot{r} = 0$, the following equation is obtained for the minimum and maximum values of r:

$$\left(\frac{r_0}{r}\right)^2 = \left(\frac{v_0}{v_{t0}}\right)^2 + 2\left(\frac{\sigma_{\rm r}}{v_{t0}}\right)^2 \left[\ln\left(\frac{\rho}{\rho_0}\right) + \beta \ln\left(\frac{r}{r_0}\right)^2\right]. \quad (17)$$

Simple iteration of this equation quickly finds the minimum orbital radius (pericentre).

For each value of r_0, we draw 10 000 velocities with the appropriate Gaussian distributions in each of the radial and tangential directions, then solve for the pericentric radius. An example histogram is shown in Fig. 11. The sharp spike at $r_{\min} = r_0$ is because any orbit that has an initial radial velocity close to zero and a tangential velocity that exceeds the circular velocity at that radius will already be at pericentre. More importantly, there is a wide distribution of minimum radii extending all the way down to $r_{\min} \approx 0$, even for an isotropic velocity dispersion tensor. This orbital distribution is in good agreement with that found in cosmological simulations, for example by Ghigna et al. (1998).

The variation in threshing radii for different galaxies is small and so for simplicity we adopt a constant value of 30 kpc. Then, for each radius, r, we can tabulate the fraction of orbits that pass within this radius. This can then be projected along the line-of-sight with the appropriate density weighting to determine the fraction of threshed orbits as a function of projected distance from the cluster centre. The results of this calculation are shown in Fig. 12 for the two example density profiles discussed above.

It is immediately apparent that the predicted fraction of threshed galaxies is far too low at radii greater than about 50 kpc. The predicted UCD fraction drops rapidly at this radius, whereas the observed fraction of UCDs stays high out to 250 kpc. (We have checked that this conclusion is unaltered even if the UCDs are distributed on a plane perpendicular to the line-of-sight such that their projected radii are equal to the true distances from the centre of the cluster.) There are many simplifications and uncertainties in the model, but it is hard to see how these could make a difference of a factor of 5. The static threshing model is simply untenable.
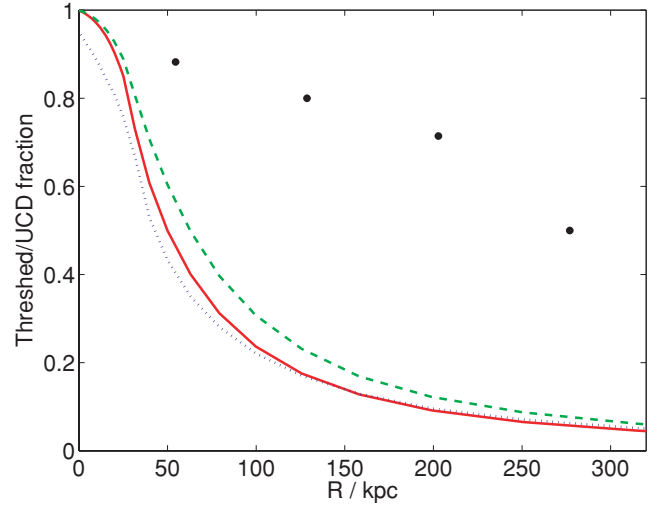
6 SUMMARY AND CONCLUSIONS

In this paper, we have investigated the possibility that UCD galaxies are formed by the threshing of nucleated, early-type dwarf galaxies.

We first contrast the distribution of nucleated and non-nucleated dwarfs, which are indistinguishable apart from a small excess of bright, nucleated dwarfs at small clustocentric radii. We concur with the conclusion of CPF06 that the observations are consistent with a single population in which all dwarfs are nucleated, with a ratio of nuclear to total magnitude that varies slowly with magnitude. However, we need to flatten their relation in order to obtain a good fit when extrapolating to fainter magnitudes.

Given this hypothesis, we can reproduce the magnitude distribution of the UCD population, except at bright magnitudes where the model predicts more UCDs than are observed. Under the threshing model, the UCDs are likely to have originated from dwarfs with magnitudes brighter than about $M_B = -15$. We use the joint UCD plus bright dwarf population in the modelling that follows.

The threshing model predicts that over half of all dwarf galaxies must be disrupted: 38 surviving dwarfs have nuclei of similar magnitude to the 49 observed UCDs. This may seem excessive but corresponds to an intracluster light fraction of just 8 per cent, well within the observed range for clusters of this mass (Feldmeier et al. 2004a,b; Gonzalez et al. 2005; Zibetti et al. 2005).

The distribution of dwarf galaxies in Fornax follows that of the total mass distribution and shows no evidence for disruption of dwarfs near the cluster core. Nevertheless, the UCD population is more centrally concentrated than the dwarfs, as would be expected in the threshing model. If we assume that the joint population is in a steady state dynamically, then it should also satisfy the Jeans equations. We show that the joint population is well-described by a density distribution of the form

$$\rho = \frac{\rho_0}{x \, (1+x)^{s-1}}, \quad (18)$$

where $x = r/a$, and a and s are constants, with s lying between about 3 and 4.5.

The velocity dispersion of UCD galaxies shows a sharp decline with radius that is hard to explain. It may in part be due to a radial bias in the orbits, but this is not enough in itself to explain the effect. The velocity dispersion of bright dwarfs is greater than that of the UCDs. When the two are combined, then the joint population with density slope $s = 3$ provides a marginally acceptable fit to the mass profile of Fornax.

We have tested the simplest possible threshing model, in which dwarf galaxies move on orbits in a static cluster potential and are threshed if they pass within a radius at which the tidal force from the cluster exceeds the internal gravity at the core of their dark matter halo. This fails to reproduce the observed fraction of UCDs at radii greater than 50 kpc from the core of Fornax. There are many deficiencies in the model but these are unlikely to raise the threshing radii by a factor of 5, as is required, and so we conclude that this static mode is unviable.

Our results have several points of agreement with the earlier work by Bekki et al. (2003) despite a very different approach: we have used analytic descriptions of the cluster dynamics compared to their numerical computations. In our work, we have based our prediction on a parent sample of dwarf galaxies generated directly from the known Fornax galaxies, whereas Bekki et al. generated their galaxy sample from more general empirical relations for the luminosity functions and radial profiles of galaxies within clusters. In particular, they used a King profile with a core radius of 50 kpc for the density distribution, very different from our model. They demonstrate that dwarf galaxies are disrupted if they pass inside their critical threshing radius when orbiting the cluster centre. They then use this radius to estimate the population of threshed galaxies (UCDs) in the Fornax cluster. They find this to be consistent with the known distribution of the seven very luminous UCDs known in the cluster at that time.

Our conclusion (refuting the simple threshing model) differs from that of Bekki et al. for a number of reasons. First, we use the measured positions of galaxies in Fornax, rather than a generic King model. We also have many fewer dwarf galaxies than predicted by their Schechter model for the cluster luminosity function. In addition, we have extended the analysis to much lower luminosities of both the UCDs (as new data have become available) and the parent galaxies (due to the greater difference in nuclear to total luminosity now used). This new analysis has clearly revealed a disagreement between the number of UCDs at large clustocentric distances and the threshing predictions.

A recent paper by GMK08 undertook an extensive series of simulations to investigate the disruption of UCD host galaxies within a cluster potential similar to that of the Virgo cluster. They considered two different models for the host galaxy with very different degrees of central concentration and followed their threshing in a static potential over 5 Gyr. They then looked at the orbits of particles in a cosmological simulation of cluster formation to assess which of those orbits would lead to threshing. This latter step follows the dynamical evolution of the halo and is much more realistic than a static potential.

GMK08 state that their model 'leads to the observed spatial distribution of UCDs', in apparent disagreement with our results above. In fact, our theoretical UCD fractions as a function of radius agree with theirs and are bracketed by their upper and lower predictions. The difference in the conclusion arises from the very different observed threshing fractions that we adopt. GMK08 use only 15 UCDs in both Virgo and Fornax combined, whereas we use a new sample of 49 UCDs from Fornax alone. Also, GMK08 do not say how they define the nucleated dwarfs corresponding to the parent sample,

whereas we are careful to select only those dwarfs that would have nuclei that match those of the observed UCDs.

In conclusion, the origin of UCDs as dwarf galaxy nuclei remains unproven. Our modelling has revealed a number of attractive features:

The distribution of nuclear magnitudes for dwarf galaxies roughly matches that of known UCD galaxies.

UCDs are more centrally concentrated within Fornax than are dwarf galaxies. (However, this would also be true if the UCDs constituted an extended globular cluster population around NGC 1399.)

The joint UCD plus bright dwarf population has a smooth density profile with a recognisable (NFW) form and appears to sit in dynamical equilibrium within the Fornax cluster.

At the same time, there are several major deficiencies in the model:

The model requires that more dwarf galaxies must have been disrupted in Fornax than currently remain. However, the spatial distribution of dwarfs matches that of the total mass profile of the cluster and shows no sign of galaxy disruption near the cluster core.

The very low velocity dispersion of UCDs as compared to bright dwarfs is unexplained, as is the sharp decline in velocity dispersion of the UCDs with radius. (However, this would prove true for any dynamical model of the UCD population, regardless of its origin.)

A static threshing model for UCD formation, based upon orbits within the current cluster potential, is a hopeless failure. It predicts far too few UCDs at radii greater than about 30 kpc.

The simulations of GMK08 within an evolving cluster potential also give too few UCDs at large radii.

The balance of evidence would seem to be against the threshing model. Before dismissing the model altogether, however, we note that the threshing may have occurred within smaller sub-clusters that later fell into Fornax and have not yet reached dynamical equilibrium. This mechanism is suggested by the spatial distribution of UCDs in the Fornax cluster: they show some association with normal galaxies and, in particular, lie in a band across the cluster (Gregg et al. 2008).

In considering the threshing hypothesis for UCD formation, we should not discuss the dynamical properties of the objects in isolation from their internal properties. Evstigneeva et al. (2007) studied the stellar populations of Virgo cluster UCDs and concluded that the Virgo UCDs have stellar populations the globular clusters of the central galaxies M87 and M49 (old ages, a range of metallicity and super-solar alpha-abundances). On this basis, the Virgo UCD stellar populations are not consistent with simple threshing model. On the other hand, Mieske et al. (2006) found metallicities and (a range of) ages in Fornax cluster UCDs, which are more in agreement with the hypothesis that the Fornax UCDs are threshed nuclei. A detailed analysis of the structure and colours of both Virgo and Fornax UCDs (Evstigneeva et al. 2008) concluded that their structural properties could be consistent with either globular clusters or dwarf galaxy nuclei, with the interesting observation that UCDs are about twice as extended (in effective radius) as the nuclei of dwarf galaxies at the same luminosity.

Most of these observational results, as well as our own analysis in this paper, argue against the simple threshing hypothesis for UCD formation.

ACKNOWLEDGMENTS

REFERENCES

Arnaboldi M., Gerhard O., Aguerri J. A. L., Freeman K. C., Napolitano N. R., Okamura S., Yasuda N., 2004, ApJ, 614, L33

Bekki K., Couch W. J., Drinkwater M. J., 2001, ApJ, 552, L105

Bekki K., Couch W. J., Drinkwater M. J., Shioya Y., 2003, MNRAS, 344, 399

Binggeli B., Tammann G. A., Sandage A., 1987, AJ, 94, 251

Blair M., Gilmore G., 1982, PASP, 94, 742

Burkert A., 1995, ApJ, 447, L25

Côté P. et al., 2006, ApJS, 165, 57 (CPF06)

Drinkwater M. J. et al., 2000a, A&A, 355, 900

Drinkwater M. J., Jones J. B., Gregg M. D., Phillipps S., 2000b, PASA, 17, 227

Drinkwater M. J., Gregg M. D., Colless M., 2001a, ApJ, 548, L139

Drinkwater M. J., Gregg M. D., Holman B. A., Brown M. J. I., 2001b, MNRAS, 326, 1076

Drinkwater M. J., Gregg M. D., Hilker M., Bekki K., Couch W. J., Ferguson H. C., Jones J. B., Phillipps S., 2003, Nat, 423, 519

Drinkwater M. J., Gregg M. D., Couch W. J., Ferguson H. C., Hilker M., Jones J. B., Karick A., Phillipps S., 2004, PASA, 21, 375

Durrell P. R., Ciardullo R., Feldmeier J. J., Jacoby G. H., Sigurdsson S., 2002, ApJ, 570, 119

Evstigneeva E. A., Gregg M. D., Drinkwater M. J., Hilker M., 2007, AJ, 133, 1722

Evstigneeva E. A. et al., 2008, AJ, 136, 461

Feldmeier J. J., Ciardullo R., Jacoby G. H., Durrell P. R., 2004a, ApJ, 615, 196

Feldmeier J. J., Mihos J. C., Morrison H. L., Harding P., Kaib N., Dubinski J., 2004b, ApJ, 609, 617

Ferguson H. C., 1989, AJ, 98, 367

Ferguson H. C., Sandage A., 1989, ApJ, 346, L53

Geha M., Guhathakurta P., van der Marel R. P., 2003, AJ, 126, 1794

Ghigna S., Moore B., Governato F., Lake G., Quinn T., Stadel J., 1998, MNRAS, 300, 146

Goerdt T., Moore B., Kazantzidis S., Kaufmann T., Macci A. V., Stadel J., 2008, MNRAS, 385, 2136 (GMK08)

Gonzalez A. H., Zabludoff A. I., Zaritsky D., 2005, ApJ, 618, 195

Gregg M. D. et al., 2008, AJ, submitted

Hilker M., Infante L., Vieira G., Kissler-Patig M., Richtler T., 1999, A&AS, 134, 75

Ikebe Y. et al., 1996, Nat, 379, 427

Irwin J. O., 1942, J. R. Stat. Soc., 105, 115

Jones C., Stern C., Forman W., Breen J., David L., Tucker W., Franx M., 1997, ApJ, 482, 143

Karick A. M., Drinkwater M. J., Gregg M. D., 2003, MNRAS, 344, 188

Mieske S., Hilker M., Infante L., Jordán A., 2006, AJ, 131, 2442

Minniti D., Kissler-Patig M., Goudfrooij P., Meylan G., 1998, AJ, 115, 121

Navarro J. F., Frenk C. S., White S. D. M., 1997, ApJ, 490, 493

Phillipps S., Drinkwater M. J., Gregg M. D., Jones J. B., 2001, ApJ, 560, 201

Pryor C., Meylan G., 1993, in Djorgovski S. G., Meylan G., eds, ASP Conf. Ser. Vol. 50, Structure and Dynamics of Globular Clusters. Astron. Soc. Pac., San Francisco, p. 357

Richtler T. et al., 2004, AJ, 127, 2094

Zibetti S., White S. D. M., Schneider D. P., Brinkmann J., 2005, MNRAS, 358, 949

APPENDIX A: TABLES OF GALAXY AND UCD DATA

Tables A1 and A2 are given in the online version of the article.

APPENDIX B: VARIATION IN LINE-OF-SIGHT VELOCITY WITH RADIUS

This Appendix calculates the expected variation in the line-of-sight velocity dispersion of UCDs with radius resulting from anisotropic motions in a declining density profile.

We take the velocity dispersion tensor to be aligned with the radial direction and to have diagonal components σ_r, σ_t and σ_t, where σ_r and σ_t are the radial and tangential components of velocity dispersion, respectively. The velocity anisotropy parameter is defined as $\beta = 1\sigma_t^2/\sigma_r^2$ – thus $\beta = 0$ for isotropic orbits and $\beta > 0$ for preferentially radial orbits. We assume that both σ_r^2 and β are constant throughout the cluster. In practice, one might expect some radial variation in these quantities, but the data are insufficient to constrain more complex models.

The line-of-sight velocity dispersion σ_{LOS} at a given projected radius R is then given by a density-weighted integral along the line of sight:

$$\sigma_{los}^2(R) = \frac{\int_0^\infty \rho(r)(\sigma_r^2 \sin^2\theta + \sigma_t^2 \cos^2\theta)\mathrm{d}z}{\int_0^\infty \rho(r)\mathrm{d}z} \tag{B1}$$

$$= \sigma_r^2 \left[1 - \beta \frac{\int_0^\infty \rho(r)\cos^2\theta\,\mathrm{d}z}{\int_0^\infty \rho(r)\,\mathrm{d}z} \right] \tag{B2}$$

$$= \sigma_r^2 \left[1 - \beta \frac{\int_0^{\pi/2} \rho(r)\,\mathrm{d}\theta}{\int_0^{\pi/2} \frac{\rho(r)}{\cos^2\theta}\,\mathrm{d}\theta} \right], \tag{B3}$$

where z measures distance along the line of sight from the mid-point through the cluster and r is the radius to a point on that line such that $z = R\tan\theta$ and $r = R/\cos\theta$. The value of the integral quotient in equation (B3) varies between approximately 0.62 and 0.76 for inner and outer radial bins given in Table 3 (the precise values depend upon the density model for the UCDs but all acceptable fits to the data give similar results).

SUPPORTING INFORMATION

Additional Supporting Information may be found in the online version of this article.

Table A1. The galaxy sample.

Table A2. The UCD sample.

Please note: Blackwell Publishing are not responsible for the content or functionality of any supplementary materials supplied by the authors. Any queries (other than missing material) should be directed to the corresponding author for the article.

This paper has been typeset from a TeX/LaTeX file prepared by the author.